Journal of
Materials Chemistry C

ROYAL SOCIETY OF CHEMISTRY

COMMUNICATION

View Article Online
View Journal | View Issue

Check for updates

Cite this: J. Mater. Chem. C, 2018, 6, 713

Received 18th September 2017,
Accepted 22nd November 2017

DOI: 10.1039/c7tc04255h

rsc.li/materials-c

Ultra-broadband and highly responsive photodetectors based on a novel $EuBiTe_3$ flake material at room temperature†

Yingying Niu, Biao Wang,* Jiapeng Chen and Dong Wu*

We report a broadband photodetector based on the novel material $EuBiTe_3$. The devices are operated at room temperature in the wavelength range from ultraviolet (370 nm) to near-infrared (1550 nm) with good reproducibility. Our results showed photoconductive responsivities greater than 1 A W^{-1} in the ultraviolet, visible and near-infrared region and the response time is recorded to be as fast as about 40 ms.

Currently, the detection of electromagnetic radiation is a key issue in research and technological development, and broadband photodetection is central to various technological applications including imaging, remote sensing, optical communications, analytical applications and military surveillance.[1–5] On account of its unique gapless electronic structure, graphene has been theoretically predicted to be a promising candidate material for broadband photodetection.[6–9] However, pure-graphene photodetectors suffer seriously from low absorption (~2.3%) and ultrafast recombination of carriers, which limits their photoresponsivity to just several mA W^{-1}.[10,11] Different methods including hybridization of quantum dots, integration of a waveguide, and plasmonic and band engineering have been exploited for improving the device performance[12–14] But the fabrication processes are very complex, which limits their mass production and most practical applications. In addition, most commercial photodetectors that operate in the visible or near-IR (NIR) region are based on silicon. However, Si photodetectors can only detect photons up to about 1110 nm owning to their finite bandgap (1.12 eV). Thus, the demand for exploring new materials which are favorable for both broadband and high performance photodetection is becoming increasingly eminent.

Here, we report a broadband photodetector based on the quasi-two-dimensional chalcogenide of $EuBiTe_3$, which was recently developed.[15] The devices are operated at room temperature in the wavelength range from UV (370 nm) to NIR (1550 nm) with good reproducibility. Our results showed photoconductive responsivities greater than 1 A W^{-1} in the UV, visible light and NIR region and the response time is recorded to be as fast as about 40 ms. Furthermore, in the absence of encapsulation, our detector suffers no obvious degradation after long-time exposure to atmosphere. We demonstrate that $EuBiTe_3$ photodetectors are able to be stably operated at room temperature as high-performance broadband photodetectors.

The $EuBiTe_3$ samples were prepared using the flux method and the parameters of the growth process were described in detail elsewhere.[15] The average size of the bulk crystals was 3 mm × 3 mm × 0.5 mm. We fabricated our photodetectors directly on $EuBiTe_3$ flakes with a thickness of 50 μm, which were exfoliated from the bulk crystals by means of the scotch tape method. Then the Au electrodes of 1 mm in length were deposited on the $EuBiTe_3$ surface by the thermal evaporation method. Finally, the $EuBiTe_3$ flakes were processed into rectangles with a photosensitive area of 0.12 mm × 1 mm.

Illuminations with wavelengths of 370 nm, 635 nm, 1064 nm and 1550 nm were generated from semiconductor lasers. The electrical characteristics of the $EuBiTe_3$ photodetector were evaluated using a Keithley 4200-SCS semiconductor parameter analyzer. All the photocurrent characteristics were analyzed under ambient conditions at room temperature.

Energy-dispersive spectroscopy (EDS), and X-ray diffraction (XRD) were conducted to study the constituents, structure and crystal quality of the flux-grown $EuBiTe_3$ flakes. EDS analysis (ESI,† Fig. S1) suggests that the components of the flakes deviate from the ideal stoichiometric ratio, with a deficiency of Bi atoms. According to previous studies,[15] this is due to the partial occupancy character for Bi elements. The XRD patterns of the $EuBiTe_3$ flakes are shown in Fig. 1(a). The sharp diffraction patterns of the (00*k*) series characterized the cleaved flakes well in the *ab*-planes, indicating that our $EuBiTe_3$ crystal samples are of high crystal quality. The inset shows that the $EuBiTe_3$ crystallizes in the orthorhombic crystal system with layered

State Key Laboratory of Optoelectronic Materials and Technologies, School of Materials, Sun Yat-sen University, Guangzhou 510275, P. R. China. E-mail: wangbiao@mail.sysu.edu.cn, wudong2@mail.sysu.edu.cn

† Electronic supplementary information (ESI) available. See DOI: 10.1039/c7tc04255h

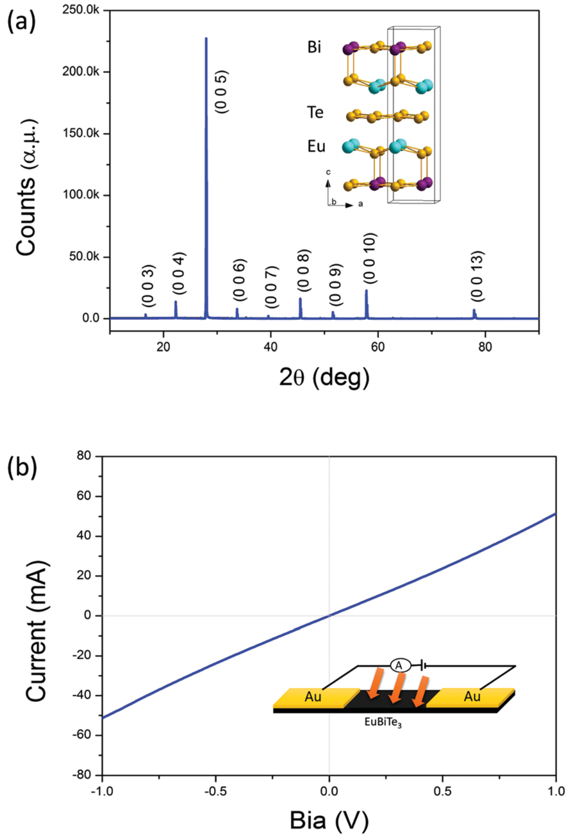

Fig. 1 The crystal structure and electronic characteristics of $EuBiTe_3$. (a) X-Ray diffraction patterns of $EuBiTe_3$ flakes. The inset shows the crystal structure of $EuBiTe_3$. (b) The typical current–voltage curves of the $EuBiTe_3$ detector. The inset shows a schematic diagram of the $EuBiTe_3$ photodetectors.

Eu–Te–Bi slabs and Te monolayer stacking along the *c*-axis direction. A schematic diagram of a typical $EuBiTe_3$ photodetector is depicted in the inset of Fig. 1(b). The device consists of a $EuBiTe_3$ flake and two Au electrodes. The Au electrodes were deposited on the $EuBiTe_3$ surface by the thermal evaporation method. Fig. 1(b) shows the typical current–voltage (*I–V*) curves of our devices at room temperature (RT). Ohmic contact between the electrodes and the $EuBiTe_3$ flake is observed from Fig. 1(b), which can ensure that the intrinsic photoresponse from the $EuBiTe_3$ flakes is acquired instead of the effect of a hetero-junction between the flakes and the Au electrodes. Besides, as the current under illumination is symmetric, the possible photovoltaic effect in the devices can be excluded[16,17] Therefore, the architecture of our detectors is proposed to be of photoconductive type.

Fig. 2 summarizes the photoresponse of the $EuBiTe_3$ photodetector for NIR(1550 nm) for instance. The switching behavior is clearly observed in Fig. 2(a). The device generates significant photocurrent under periodic illuminations. We can see that the photocurrent ramps to a high level under illumination and annihilates after removing the illumination. Fig. 2(b) shows the decay time of the photodetector and the saturation time is shown in the inset of Fig. 2(b). For decay time analysis, the two-component decay function was used:

$$I_t = I_1 e^{-t/\tau_1} + I_2 e^{-t/\tau_2}$$

where I_t is the normalized decaying photocurrent, and t is the time after switching off the illumination. Two different decay components were found, with the fast one being below 40 ms and the slow one being at a magnitude of around $\sim$1 s. The intensity of the slow one I_2 contributed a small part (13%) to the decay process for our measurements. On the one hand, we ascribed the I_2 component to the background bolometric effect due to the heat exchange between the device and the surroundings during experiments (considering the bad-heat conductance between the devices and their surroundings, *i.e.* atmosphere or glass-substrates, the decay time of the bolometric effect will

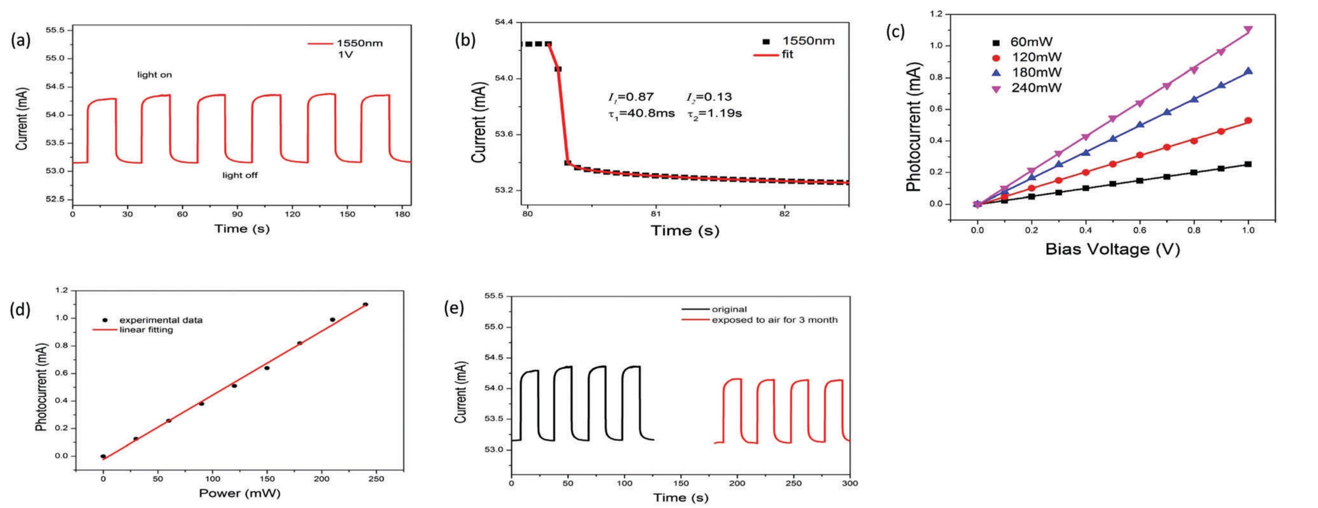

Fig. 2 The performances of the $EuBiTe_3$ photodetector. (a) Time-dependent switching behavior of the photocurrent. Device area: 1 mm × 0.12 mm, power density: 490 mW cm^{-2}. (b) The photoresponse decay process of our detectors (bottom panel) under lasers at wavelengths of 1550 nm. Two decay components were found at each case, with the fast one (τ_1) about 40 ms and the slow one (τ_2) around the order of $\sim$1 s. (c) Voltage-dependent photocurrent at various light intensities. (d) Power-dependent photocurrent. Source–drain voltage: 1 V. (e) Stability of the $EuBiTe_3$ photodetector; red is stored in ambient environment for 3 months without any encapsulation. The curve is horizontally shifted for clarity.

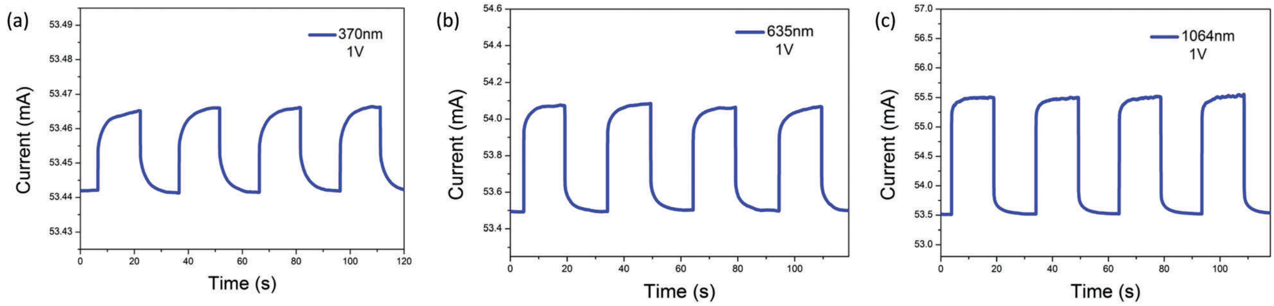

Fig. 3 Ultra-broadband photoresponse of the $EuBiTe_3$ photodetector. Time-dependent switching behavior under illumination of (a) 370 nm, power density: 70 mW cm^{-2}, (b) 635 nm, power density: 260 mW cm^{-2} and (c) 1064 nm, power density: 1.7 W cm^{-2}.

be more sensitive to the surroundings); on the other hand, the I_2 component could also be caused by the photogating effect.[18] Thus, we consider the fast one as intrinsic and estimate the response time of photo-generated carriers to be about 40 ms. Besides, the time dependence shows weak light intensity dependence (see ESI,† Fig. S2).

Fig. 2(c) and (d) show the voltage-dependent photocurrent and power-dependent photocurrent, respectively. Obviously, we can see that the photocurrent is linearly proportional to both the driving voltage and the incident power. For the driving voltage, a large external voltage can efficiently restrain the recombination of photogenerated carriers, so that carrier separation is easier. Therefore, the photocurrent increases as the voltage increases. For the incident power, a larger number of electron–hole pairs are generated under stronger illumination. The good linear relationship between photocurrent and power suggests that our device can effectively distinguish different light intensities. In general, our device can have good tunability for multi-purpose applications because of the linear dependence on both the voltage and the incident power.[19–21]

In addition, the stability is a crucial factor for the photodetector in practical applications. For example, some photodetectors based on organic materials[22,23] are not stable because of their weak oxidation resistance. Thus, the durability to oxidative degradation in an ambient environment is investigated. Fig. 2(e) shows the performance of our device before and after storage for 3 months in an ambient environment without any encapsulation; there is no obvious reduction observed between the before and after. Therefore, owing to the low chemical activity of the compound, the $EuBiTe_3$ photodetector exhibits excellent stability in an ambient environment.

The spectral response range is another important performance parameter of the photodetector. For a photoconductive detector (usually referred to as a semiconductor detector), the spectral response range is closely related to the bandwidth of the detector. On account of the narrow-gap (0.3 eV),[15] $EuBiTe_3$ is predicted to be a promising candidate material for broadband photodetection. Fig. 3 shows the broadband photoresponse of the $EuBiTe_3$ photodetector. As observed, Fig. 3(a)–(c) and Fig. 2(a) show good switching behavior under periodic illumination with different laser wavelengths (370 nm, 635 nm, 1064 nm, and 1550 nm), suggesting an ultra-broadband photoresponse range from ultraviolet to infrared for our devices.

For a photoconductive detector, the signal component of sensitivity is quantified by the current photoresponsivity (R), which is the ratio of photocurrent (I_{ph}) to the incident light power (P_{in}) and expressed as $R = I_{ph}/P_{in}$, in the units of A W^{-1}. Fig. 4(a) shows the spectral responsivity curve. The responsivity at 370 nm, 635 nm, 1064 nm and 1550 nm is 2.8 A W^{-1}, 1.9 A W^{-1}, 1 A W^{-1} and 1.7 A W^{-1}, respectively. The responsivity reaches the maximum value at 370 nm and the minimum value at 1064 nm. Interestingly, the responsivity shows weak light intensity dependence in our device (see ESI,† Table S1). From the optical absorbance spectrum of $EuBiTe_3$ crystals (Fig. 4(a)), the responsivities of different wavelengths are well consistent with the intrinsic absorption of the $EuBiTe_3$. Evidently, our devices demonstrated high responsivity in the UV, VIS and NIR range measured with magnitudes greater than 1 A W^{-1}, as

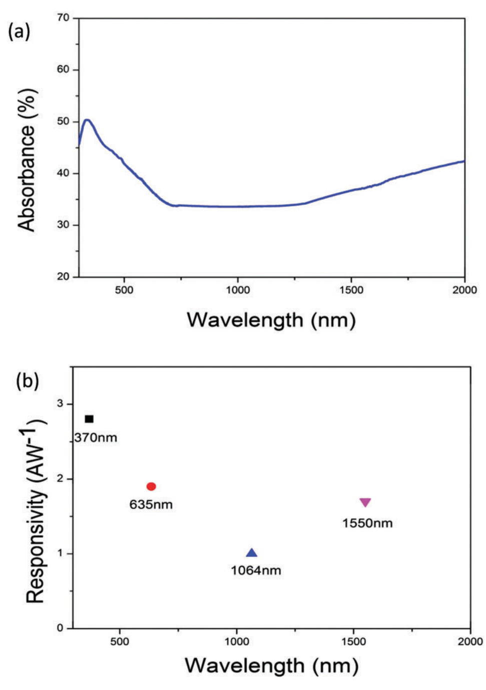

Fig. 4 Optical absorbance and responsivity characteristics for $EuSbTe_3$ detectors. (a) RT *ab*-plane optical absorbance spectrum of $EuBiTe_3$ crystals. (b) The responsivity for our $EuBiTe_3$ detectors under illumination with wavelengths from UV to NIR based on the same device. Device area: 1 mm × 0.12 mm.

required by most applications. Such broad responsivity range is attributed to the narrow band gap of the $EuBiTe_3$, as the photons from UV to NIR have enough energy to excite the electrons from the conduction band to the valence band. Our observations of the responsivities in $EuBiTe_3$ detectors far surpass the initially reported devices based on other 2D materials, such as 1 mA W^{-1} for pure graphene,[1] and 7 mA W^{-1} for MoS_2.[24] Most remarkably, compared with the traditional silicon detector, the $EuBiTe_3$ photodetector exhibited high responsivity to ultraviolet and telecommunication wavebands (λ = 370 nm, and 1550 nm) at RT. However, the extremely high dark current at the magnitude of 10^{-3} A lead to a detectivity of 0.6×10^{-9} cm $Hz^{1/2}$ W^{-1} (see ESI,† S3).

In summary, we have fabricated a photodetector based on flux-grown $EuBiTe_3$ flakes and investigated its photoresponse. We demonstrate devices with stable ultra-broadband photoresponse from 370 nm to 1550 nm with good reproducibility at room temperature. Our devices exhibited high responsivity in the range from UV to NIR with magnitudes greater than 1 A W^{-1}. In particular, the $EuBiTe_3$ photodetector exhibited high responsivity to ultraviolet and telecommunication wavebands (λ = 370 nm, and 1550 nm) at RT along with a fast decay time of ~40 ms. In addition, our devices show that the photocurrent is linearly proportional to the driving voltage and the incident power, offing good tunability for multi-purpose applications. Furthermore, our devices without any encapsulation suffer no obvious degradation after a long time period of three months of exposure to air. In general, we demonstrate that $EuBiTe_3$-based photodetectors are able to be stably operated at room temperature as high-performance broadband photodetectors.

Conflicts of interest

There are no conflicts to declare.

Acknowledgements

This work was supported by the National Natural Science Foundation (Grant No. 11472313, 11472317, 11232015 and 11572355).

References

1 T. Mueller, F. Xia and P. Avouris, Graphene photodetectors for high-speed optical communications, *Nat. Photonics*, 2010, **4**(5), 297–301.
2 A. Gassenq, F. Gencarelli and C. J. Van, *et al.*, GeSn/Ge heterostructure short-wave infrared photodetectors on silicon, *Opt. Express*, 2012, **20**(25), 27297.
3 K. T. Lin, H. L. Chen and Y. S. Lai, *et al.*, Silicon-based broadband antenna for high responsivity and polarization-insensitive photodetection at telecommunication wavelengths, *Nat. Commun.*, 2014, **5**(1), 3288.
4 S. Adhikary, Y. Aytac and S. Meesala, *et al.*, A multicolor, broadband (5–20 μm), quaternary-capped InAs/GaAs quantum dot infrared photodetector, *Appl. Phys. Lett.*, 2012, **101**(26), 261114.
5 W. Zhao, J. Lei and Y. Hang, *et al.*, Targeting human embryonic stem cells with quantum dot-conjugated phages, *Sci. Rep.*, 2013, **3**(45), 3134.
6 A. C. Ferrari, Graphene Photonics and Optoelectronics, *Nat. Photonics*, 2016, **4**(9), 611–622.
7 F. Bonaccorso, Z. Sun and T. Hasan, *et al.*, Graphene photonics and optoelectronics, *Nat. Photonics*, 2010, **4**(9), 611–622.
8 F. H. Koppens, T. Mueller and P. Avouris, *et al.*, Photodetectors based on graphene, other two-dimensional materials and hybrid systems, *Nat. Nanotechnol.*, 2014, **9**(10), 780–793.
9 N. M. Gabor, J. C. Song and Q. Ma, *et al.*, Hot carrier-assisted intrinsic photoresponse in graphene, *Science*, 2011, **334**(6056), 648.
10 K. J. Yee, J. H. Kim and M. H. Jung, *et al.*, Ultrafast modulation of optical transitions in monolayer and multilayer graphene, *Carbon*, 2011, **49**(14), 4781–4785.
11 F. Xia, T. Mueller and Y. M. Lin, *et al.*, Ultrafast graphene photodetector, *Nat. Nanotechnol.*, 2009, **4**(12), 1–2.
12 F. Wang, Y. Zhang and C. Tian, *et al.*, Gate-Variable Optical Transitions in Graphene, *Science*, 2008, **320**(5873), 206.
13 J. Bai, X. Duan and Yu Huang, Rational fabrication of graphene nanoribbons using a nanowire etch mask, *Nano Lett.*, 2009, 2083–2087.
14 J. Bai, *et al.*, Graphene nanomesh, *Nat. Nanotechnol.*, 2010, 190–194.
15 Y. Y. Niu, D. Wu and L. Shen, *et al.*, A layered antiferromagnetic semiconductor $EuMTe_3$ (M = Bi, Sb), *Phys. Status Solidi RRL*, 2015, **9**(12), 735–739.
16 Y. Wang, X. Deng and G. Zhang, *et al.*, Terahertz photodetector based on double-walled carbon nanotube macrobundle-metal contacts, *Opt. Express*, 2015, **23**(10), 13348–13357.
17 J. Tong, M. Muthee and S. Y. Chen, *et al.*, Antenna Enhanced Graphene THz Emitter and Detector, *Nano Lett.*, 2015, **15**(8), 5295.
18 C. Xie, C. Mak and X. Tao, *et al.*, Photodetectors Based on Two-Dimensional Layered Materials Beyond Graphene, *Adv. Funct. Mater.*, 2017, **27**, 19.
19 J. Yao, J. Shao and Y. Wang, *et al.*, Ultra-broadband and high response of the Bi_2Te_3-Si heterojunction and its application as a photodetector at room temperature in harsh working environments, *Nanoscale*, 2015, **7**(29), 12535.
20 J. D. Yao, J. M. Shao and G. W. Yang, Ultra-broadband and high-responsive photodetectors based on bismuth film at room temperature, *Sci. Rep.*, 2015, **5**, 12320.
21 Y. Y. Niu, D. Wu and Y. Q. Su, *et al.*, Uncooled $EuSbTe_3$ photodetector highly sensitive from ultraviolet to terahertz frequencies, *2D Mater.*, 2017, **5**(1), 011008.
22 P. E. Burrows, V. Bulovic and S. R. Forrest, *et al.*, Reliability and degradation of organic light emitting devices, *Appl. Phys. Lett.*, 1994, **65**(23), 2922–2924.
23 H. Aziz, Z. Popovic and C. P. Tripp, *et al.*, Degradation processes at the cathode/organic interface in organic light emitting devices with Mg:Ag cathodes, *Appl. Phys. Lett.*, 1998, **72**(21), 2642–2644.
24 Z. Yin, H. Li and H. Li, *et al.*, Single-layer MoS_2 phototransistors, *ACS Nano*, 2012, **6**(1), 74–80.

